



## Short Communication

Effects of ball milling on microstructure and electrical properties of sol-gel derived  $(\text{Bi}_{0.5}\text{Na}_{0.5})_{0.94}\text{Ba}_{0.06}\text{TiO}_3$  piezoelectric ceramicsHongqiang Wang<sup>a</sup>, Ruzhong Zuo<sup>a,\*</sup>, Xun Ji<sup>a</sup>, Zhengkui Xu<sup>b</sup><sup>a</sup> Institute of Electro Ceramics & Devices, School of Materials Science and Engineering, Hefei University of Technology, Hefei 230009, PR China<sup>b</sup> Department of Physics and Materials Science, City University of Hong Kong, Hong Kong, PR China

## ARTICLE INFO

## Article history:

Received 11 February 2010

Accepted 21 April 2010

Available online 24 April 2010

## ABSTRACT

A citrate sol-gel method was investigated for synthesizing lead-free piezoelectric compositions of  $(\text{Bi}_{0.5}\text{Na}_{0.5})_{0.94}\text{Ba}_{0.06}\text{TiO}_3$  (BNT) and the effect of ball milling on the sintering, microstructure and electrical properties of BNT ceramics was emphasized. The thermal analysis and X-ray diffraction results show that crystalline powders with a single perovskite structure can be obtained when calcined at 600 °C for 3 h. The average particle size of as-calcined powder and electrical properties of sintered samples were obviously dependent on an additional ball milling. Because of well-dispersed superfine powders (~100 nm), the BNT ceramics can be well densified at temperature 50 °C lower than that by mixed-oxide method and conventional sol-gel method and as a result exhibit enhanced electrical properties of a piezoelectric constant  $d_{33} \sim 180$  pC/N and a planar electromechanical coupling factor  $k_p \sim 0.29$ .

© 2010 Elsevier Ltd. All rights reserved.

## 1. Introduction

Sodium bismuth titanate  $(\text{Bi}_{0.5}\text{Na}_{0.5})\text{TiO}_3$  (BNT) is a ferroelectric composition with an  $\text{ABO}_3$  perovskite structure of A-site complex occupation that has been widely studied [1]. However, because of its high coercive field,  $E_c = 73$  kV/cm, and relatively large conductivity, pure BNT is difficult to be poled so that its practical application is limited. These problems were overcome by forming solid solutions with  $\text{BaTiO}_3$ ,  $\text{BiFeO}_3$ ,  $\text{NaNbO}_3$ ,  $\text{SrTiO}_3$ ,  $(\text{K}_{0.5}\text{Bi}_{0.5})\text{TiO}_3$ , etc. [2–7]. Among these solid solutions  $(\text{Bi}_{0.5}\text{Na}_{0.5})_{1-x}\text{Ba}_x\text{TiO}_3$  system has attracted a great deal of attention owing to the existence of a rhombohedral–tetragonal morphotropic phase boundary (MPB) near  $x = 0.06$ – $0.08$ , where the materials show significantly enhanced piezoelectric properties and reduced coercive field. Take-naka et al. [2] reported that  $(\text{Bi}_{0.5}\text{Na}_{0.5})_{0.94}\text{Ba}_{0.06}\text{TiO}_3$  (BNBT6) in the composition range of MPB has relatively good piezoelectric properties of  $d_{33} = 125$  pC/N,  $k_{31} = 0.19$  and  $k_{33} = 0.55$ . Afterwards, many attempts were made to further improve the electrical properties by substituting A-site or B-site atoms with  $\text{La}^{3+}$ ,  $\text{Nb}^{5+}$ ,  $\text{Mn}^{2+}$ ,  $\text{Co}^{3+}$ , etc. [8,9,4,10].

Similar to many other electroceramics, BNT based ceramics are usually produced by conventional mixed-oxide method [5–9,4,10]. However, a relatively high sintering temperature is needed, which tends to cause the volatilization of A-site elements [11]. By comparison, wet chemical methods exhibit many advantages such as accurate chemical stoichiometry, high composition homogeneity

and lower crystallization temperature due to the mixing of liquid precursors on the molecular level. Therefore, it can be realized to lower the sintering temperature and to further limit the loss of volatile  $\text{Bi}_2\text{O}_3$  and  $\text{Na}_2\text{O}$ . Several chemical methods, like conventional sol-gel method [12], hydrothermal method [13,14], mechanochemical synthesis [15], sol-gel auto-combustion method [16,17] and citrate method [18] have been already applied for obtaining sodium bismuth titanate based ceramics. Zhao et al. [12] reported a conventional sol-gel method to synthesize BNBT6 powders, but it is not an ideal sol-gel process because barium nitrate is insoluble in acetic acid. As a result, the final composition will be away from the stoichiometric one. This problem was expected to be improved by a citrate method. In this study, the citrate method was used to synthesize the superfine powders and the part of as-synthesized BNBT6 powder was milled for 8 h, in comparison to the rest that was not milled. In addition, the effects of ball milling on microstructure and electrical properties of the ceramics were investigated.

## 2. Experimental procedures

The raw materials used in this study are  $\text{CH}_3\text{COONa} \cdot 3\text{H}_2\text{O}$  ( $\geq 99.0\%$ ),  $\text{Bi}(\text{NO}_3)_3 \cdot 5\text{H}_2\text{O}$  ( $\geq 99.0\%$ ),  $\text{Ba}(\text{CH}_3\text{COO})_2$  ( $\geq 99.0\%$ ), tetrabutyl titanate ( $\geq 98.0\%$ ), citric acid ( $\geq 99.5\%$ ), glycol ( $\geq 99.0\%$ ) and ammonia (25–28%). The molar ratio of citric acid to metal cations was 1.2:1. The appropriate amount of citric acid was first dissolved into deionized water. Tetrabutyl titanate diluted in ethanol was then added slowly while a pH value of 7 was adjusted by dripping a small amount of ammonia. After being stirred at 80 °C for 1 h, a yellowish liquid was obtained. Various metal salts and glycol were

\* Corresponding author. Tel./fax: +86 551 2905285.

E-mail address: [piezolab@hfut.edu.cn](mailto:piezolab@hfut.edu.cn) (R. Zuo).

introduced into the solution, followed by a stirring process for 2 h to generate a stable transparent sol. Citric acid is a polydentate ligand with two carboxyls and a hydroxyl and can easily form stable and soluble chelate complexes with metal cations in an alkaline solution. Glycol with double carboxyls can form ester groups, become network structures by increasing molecular weight of precursors, and further enhance the stability of solution. The sol was heated at 100 °C to remove redundant solvent and to form gel. Subsequently, the gel was calcined at 400–600 °C for 3 h to obtain yellowish crystallite powders. Then the powders were milled for 8 h using planetary milling with zirconia ball in alcohol. The dried powders were pressed into discs and then sintered at 1070–1170 °C for 3 h in air. Fired-on silver paste was used as electrodes for the measurement of the electrical properties of sintered samples. The ceramics were poled in silicone oil under a dc electric field of 3–4 kV/mm at 60 °C for 20 min.

Thermo-gravimetry (TG) and differential scanning calorimetry (DSC) analyses of the as-prepared gel were carried out by using a simultaneous thermal analyzer (STA409C, Netzsch, Germany). The calcined powders were characterized by an X-ray diffractometer (XRD, D/Max-RB, Rigaku, Japan) and a transmission electron microscope (TEM, Model H-800, Hitachi, Japan). The microstructure of sintered samples was observed using a scanning electron microscope (SEM, SSX-550, Shimadzu, Japan). The dielectric properties were measured as a function of temperature by a LCR meter (Agilent E4980A, USA). The piezoelectric constant  $d_{33}$  was measured directly on a quasi-static  $d_{33}$  meter (YE2730A, Sinocera, China). The electromechanical coupling coefficient  $k_p$  was measured by a high precision impedance analyzer (PV70A, Beijing Band ERA Co. Ltd., China). Polarization hysteresis loops were measured under an alternating electric field using a ferroelectric measuring system (Precision LC, Radiant Technologies, Inc., USA).

### 3. Results and discussion

Fig. 1 shows TG and DSC curves of the BNBT6 gel. A small weight loss of 4.0% at temperatures up to ~165 °C is due to the evaporation of remaining water, glycol and ammonia. There is a gentle endothermic peak at ~198 °C, which is ascribed to the fusion heat of superfluous citrate acid. The exothermic peaks at ~288 °C and ~473 °C are attributed to the thermal decomposition of citrate acid and citrate complexes, corresponding to weight losses of 36.6% and 17.3%, respectively. The strong exothermic peak at 502 °C can be related to the combustion of residual organic components, accompanied by a weight loss of 14.5%. No further weight loss or peaks can be seen thereafter in the TG and DSC curves, indicating that the thermal decomposition of BNBT6 gel is completed

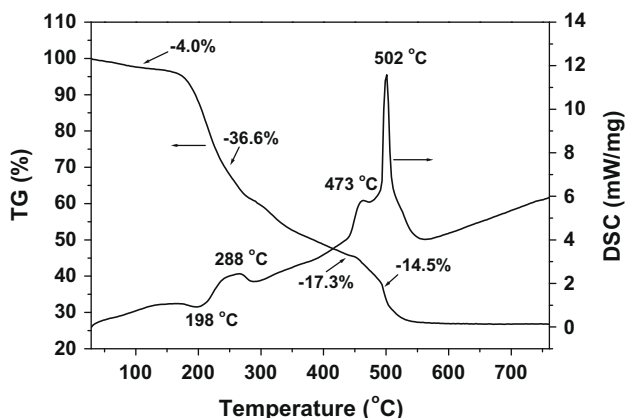


Fig. 1. TG and DSC curves of the BNBT6 gel.

before 600 °C. In addition, there should be a tiny endothermic peak in the temperature range of 400–500 °C in the DSC curve because of the crystallization of BNBT6 amorphous powders. However, this endothermic peak is invisible, probably because it was counteracted by the thermal decomposition of citrate complexes or combustion of residual organic components.

The XRD patterns of BNBT6 gel powders calcined at different temperatures in the  $2\theta$  range of 20–80° are shown in Fig. 2. The powders calcined below 400 °C exhibit typical patterns of amorphous phases. When the calcination temperature rises to 500 °C, the characteristic diffraction peaks of a perovskite structure begin to appear. A small amount of an intermediate phase (indexed as  $\text{Bi}_4\text{Ti}_3\text{O}_{12}$ ) can be observed when the gel is calcined below 600 °C.

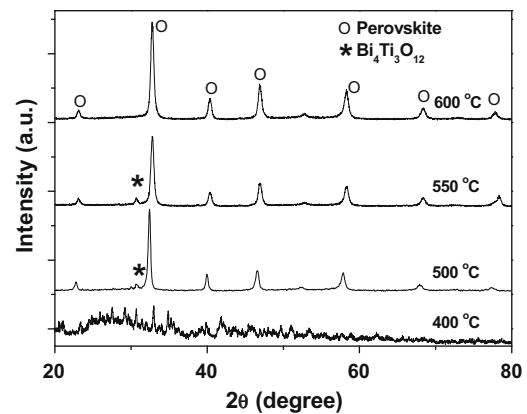


Fig. 2. XRD patterns of BNBT6 powders calcined at different temperatures.

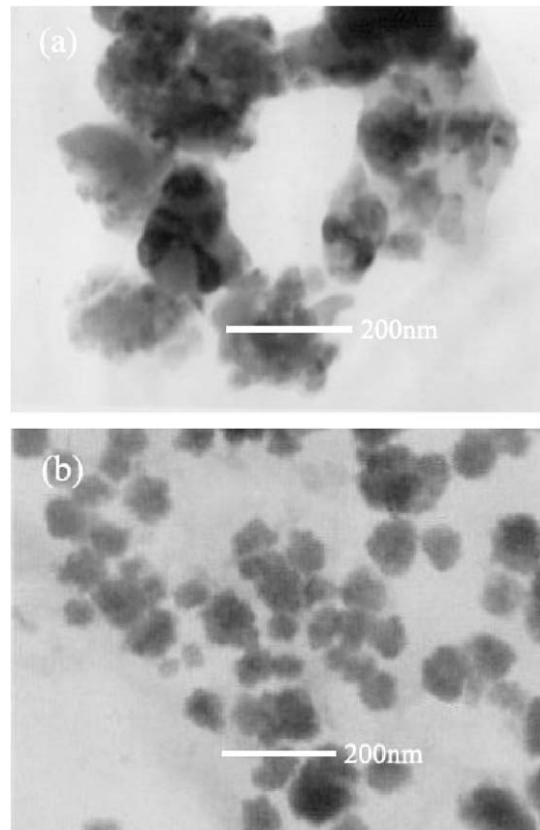


Fig. 3. TEM photograph of the BNBT6 powders calcined at 600 °C for 3 h: (a) without ball milling and (b) with ball milling.

However,  $\text{Bi}_4\text{Ti}_3\text{O}_{12}$  disappears and a single perovskite structure can be obtained when the gel is calcined at  $600^\circ\text{C}$ . The chelate complex with metal cations allows molecular level mixing during the course of forming the sol so the migration distance of various ions is much shorter than that by a mixed-oxide method during calcination. Thus, the calcination temperature of BNBT6 gel powders is approximately  $300^\circ\text{C}$  lower than those prepared by conventional mixed-oxide method.

Fig. 3 displays the TEM photographs of the BNBT6 powder calcined at  $600^\circ\text{C}$  for 3 h. The aggregate phenomenon of powders without ball milling (Fig. 3a) is serious. After milling, the crystalline particles (Fig. 3b) are well dispersed with only a slight degree of soft agglomeration and the particles are about 100 nm or less in size. Fig. 4a shows the surface morphology of the BNBT6 ceramics without ball milling sintered at  $1150^\circ\text{C}$  and Fig. 4b shows that with ball milling sintered at  $1110^\circ\text{C}$ . Both temperatures correspond to their individual optimum sintering temperatures. It is clear that the sintering temperature of the ceramics with ball milling is lower than that without ball milling and the grain size is thus reduced significantly ( $\sim 5\ \mu\text{m}$  and  $\sim 1.5\ \mu\text{m}$  for samples without ball milling and with ball milling, respectively). The density of the samples is slightly increased as well owing to an additional milling process. In addition, it can be also found that the grain morphologies change from a square pillar shape to a polyhedral shape. These results indicate that the as-prepared powders with ball milling own a good sintering activity, leading to a relatively low sintering temperature and an improved densification behavior.

Fig. 5a shows the dielectric properties at 1 kHz between BNBT6 samples with ball milling and without ball milling. Both the dielectric constant at room temperature and dielectric maxima of the ceramics with ball milling increase compared to those without ball milling, which should be mostly related to the improved densifica-

tion behavior. The dielectric properties at different frequencies of sintered samples prepared with ball milling are shown in Fig. 5b. It is obvious that there exist ferroelectric, anti-ferroelectric and paraelectric phases in different temperature ranges, which are in good agreement with those reported by Takenaka et al. [2,10].  $T_d$  refers to the transition temperature between ferroelectric phase and anti-ferroelectric phase and  $T_m$  represents the temperature at which the dielectric constant  $\epsilon_r$  reaches the maximum. It can be seen that both  $\epsilon_r$  and loss value  $\tan\delta$  are strongly frequency dependent near  $T_d$ . At  $T_m$ , the ceramics exhibit a diffuse phase transition behavior. These indicate that BNBT6 ceramics are relaxor-like, which could be associated with the complex occupation of  $\text{Ba}^{2+}$ ,  $\text{Na}^+$  and  $\text{Bi}^{3+}$  cations at A-sites.

The polarization versus electric field (P–E) hysteresis loops of BNBT6 ceramics prepared via different processes are shown in Fig. 6. A comparison of P–E hysteresis loops between samples with ball milling and without ball milling is shown in Fig. 6a. The remnant polarization  $P_r$  of the BNBT6 ceramics increases from  $32.1$  to  $36.1\ \mu\text{C}/\text{cm}^2$  and the coercive field  $E_c$  decreases from  $2.79$  to  $2.61\ \text{kV}/\text{mm}$  after ball milling. The sintering temperature of ceramics without ball milling is relatively high, so the oxygen vacancy can be more seriously generated by the volatilization of bismuth and thus inhibits the domain movement, which causes a slight increment of  $E_c$ . The relevant reason for the decreased  $P_r$  (or saturated polarization) could be related to the changed grain size as well. The more fraction of grain boundary for samples with small grain size might reduce the value of electric field loaded on the grains. Furthermore, the  $E_c$  value of BNBT6 ceramics prepared via a sol–gel route is much lower than that of BNBT6 ceramics made

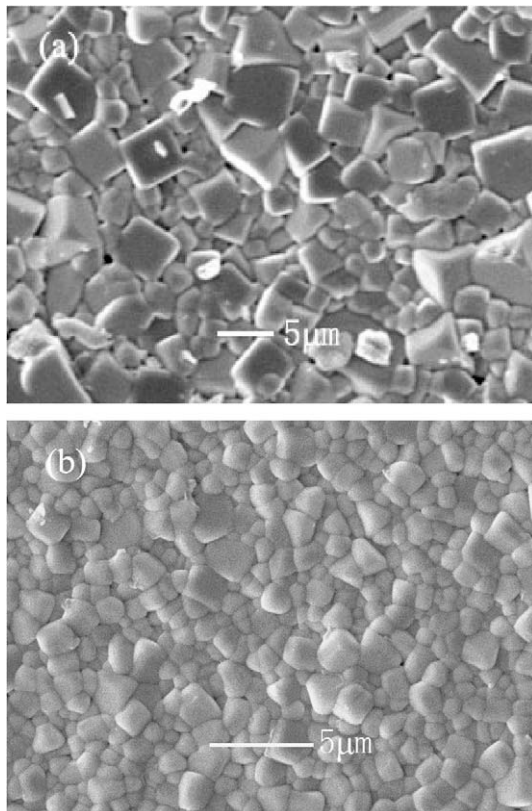


Fig. 4. SEM image of BNBT6 ceramics sintered at 1150 and 1110 °C: (a) without ball milling and (b) with ball milling.

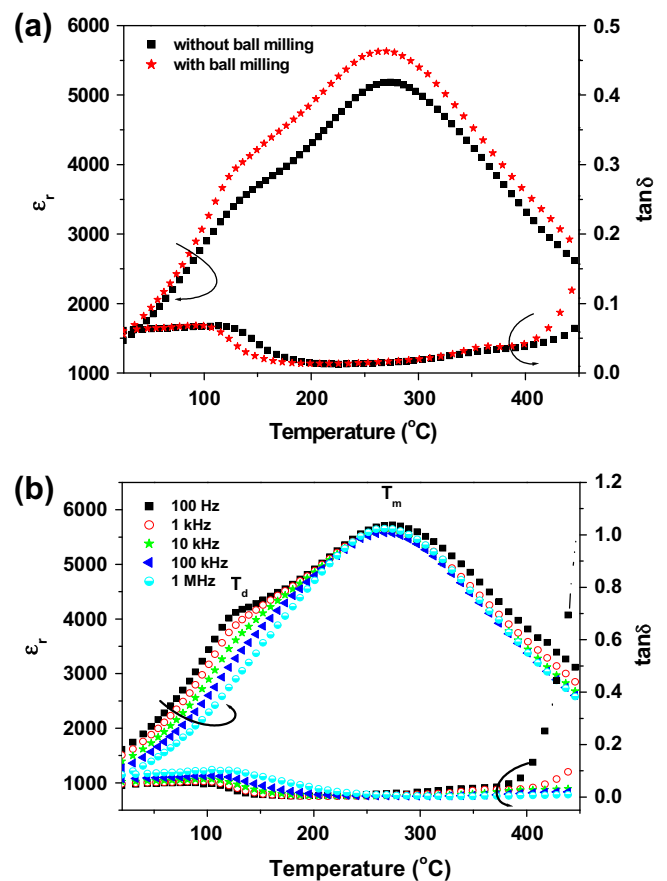
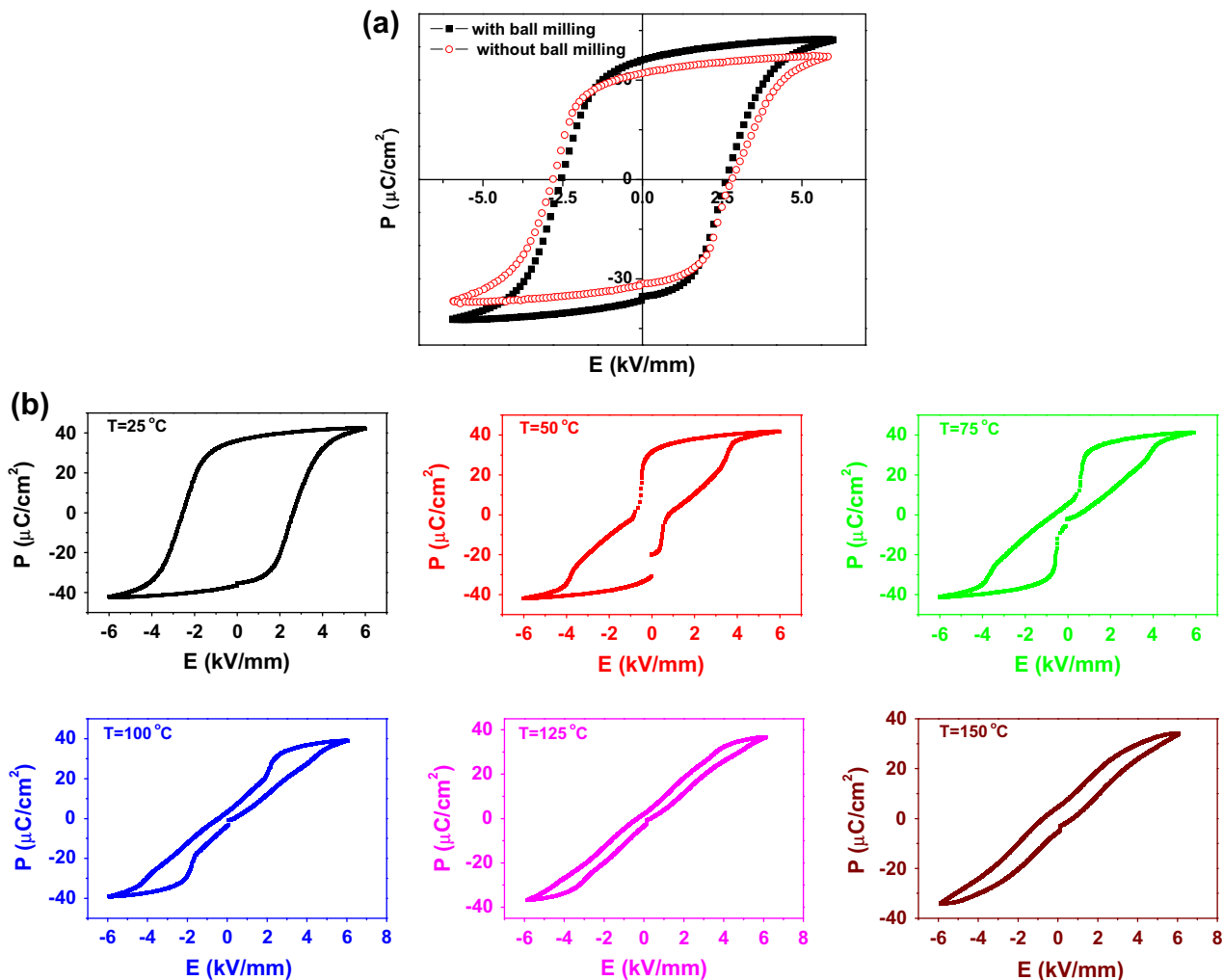


Fig. 5. (a) The dielectric properties at 1 kHz between BNBT6 samples with ball milling and without ball milling and (b) the dielectric properties at different frequencies for sintered samples prepared with ball milling.



**Fig. 6.** P–E hysteresis loops of BNBT6 ceramics prepared via different processes: (a) a comparison of P–E hysteresis loops between samples with ball milling and without ball milling and (b) for samples prepared with ball milling at various measuring temperatures.

by a mixed-oxide method [19]. The lower  $E_c$  tends to facilitate the domain movement and thereby enhances piezoelectric properties. Fig. 6b displays the P–E hysteresis loops of BNBT6 ceramics with ball milling at various measuring temperatures. At room temperature, BNBT6 ceramics are typically ferroelectric, while they exhibit double hysteresis loops typical for an anti-ferroelectric phase with the increase of temperature owing to the rhombohedral ferroelectric to tetragonal anti-ferroelectric phase transition. In addition, it can be seen that anti-ferroelectric phases exhibit higher forward switching electric field with increasing the measuring temperature because of enhanced stability of anti-ferroelectric phases. Therefore, P–E loops at various temperatures demonstrate that the transition from ferroelectric to anti-ferroelectric phases exists at  $T_d$  as mentioned in Fig. 5b. Unfortunately, the existence of  $T_d$  could limit the application of this piezoelectric composition because of the depolarization above  $T_d$ . It was also indicated that the  $T_d$  value can be shifted downward by a few dopants [8,9,4,10]. How the  $T_d$  value can be significantly increased has been a key issue of this composition for the final application.

Table 1 shows a comparison of sintering temperature, dielectric and piezoelectric properties of BNBT6 ceramics prepared using different synthesis methods. It is clear that the piezoelectric and dielectric properties obtained in this study are superior to those prepared by mixed-oxide and traditional sol–gel methods. In addition,

**Table 1**

Sintering temperature, dielectric and piezoelectric properties of BNBT6 ceramics prepared with different synthesis methods.

Processing	Sintering temperature (°C)	$d_{33}$ (pC/N)	$k_p$	$\tan \delta$	$\epsilon_{33}^T$
Mixed-oxide method [2]	1200	125	–	0.013	580
Conventional sol–gel method [8]	1160	173	0.26	0.039	820
Citrate method with ball milling [this study]	1110	180	0.29	0.035	870
Citrate method without ball milling [this study]	1150	168	0.27	0.049	830

tion, after ball milling the sintering temperature is lowered by 50 °C or more. The ceramics prepared by the citrate method exhibit excellent piezoelectric properties of  $d_{33} \sim 180$  pC/N, which could be related to the high chemical homogeneity and a dense fine microstructure. The precipitation of barium nitrate in the traditional sol–gel method was solved successfully by the citrate method and a real molecular-level complete mixing can be achieved. Furthermore, the sintering temperature can be lowered down to 1110 °C as a result of the high sintering activity from superfine powders.

#### 4. Conclusions

A citrate wet chemical processing route was investigated in order to synthesize BNBT6 superfine powders. The effect of ball milling on the sintering, microstructure and electrical properties of BNT ceramics was emphasized. The gel can be transformed into crystalline powders with a pure perovskite structure after heat treatment at 600 °C for 3 h and the particle size of the powder through an additional ball milling is about 100 nm. The ceramics have a dense fine microstructure and excellent piezoelectric and dielectric properties when sintered at a relatively low temperature compared with those prepared by mixed-oxide method or traditional sol–gel method.

#### Acknowledgements

This work was financially supported by a project of Natural Science Foundation of Anhui Province (090414179), by the National Natural Science Foundation of China (50972035) and a Program for New Century Excellent Talents in University, State Education Ministry (NCET-08-0766) and also partially supported by a grant from the Research Grants Council of the Hong Kong Region, China (No. CityU 103307).

#### References

- [1] Xu Q, Chen XL, Chen W, Chen ST, Kim B, Lee J. Synthesis, ferroelectric and piezoelectric properties of some  $(\text{Na}_{0.5}\text{Bi}_{0.5})\text{TiO}_3$  system compositions. *Mater Lett* 2005;59:2437–41.
- [2] Takenaka T, Maruyama K, Sakata K.  $(\text{Na}_{0.5}\text{Bi}_{0.5})\text{TiO}_3$ – $\text{BaTiO}_3$  system for lead-free piezoelectric ceramics. *Jpn J Appl Phys* 1991;30:2236–9.
- [3] Senda S, Jean-Pierre M. Relaxor behavior of low lead and lead free ferroelectric ceramic of the  $(\text{Na}_{0.5}\text{Bi}_{0.5})\text{TiO}_3$ – $\text{PbTiO}_3$  and  $(\text{Na}_{0.5}\text{Bi}_{0.5})\text{TiO}_3$ – $(\text{K}_{0.5}\text{Bi}_{0.5})\text{TiO}_3$  systems. *J Eur Ceram Soc* 2001;21:1333–6.
- [4] Li HD, Feng CD, Yao WL. Some effects of different additives on dielectric and piezoelectric properties of  $(\text{Bi}_{0.5}\text{Na}_{0.5})\text{TiO}_3$ – $\text{BaTiO}_3$  morphotropic phase boundary composition. *Mater Lett* 2004;58:1194–8.
- [5] Takenaka T, Okuda T, Takegahara K. Lead-free piezoelectric ceramics based on  $(\text{Bi}_{0.5}\text{Na}_{0.5})\text{TiO}_3$ – $\text{NaNbO}_3$ . *Ferroelectrics* 1997;196:175–8.
- [6] Nagata H, Koizumi N, Takenaka T. Lead-free piezoelectric ceramics of  $(\text{Bi}_{0.5}\text{Na}_{0.5})\text{TiO}_3$ – $\text{BiFeO}_3$ -system. *Key Eng Mater* 1999;169:37–40.
- [7] Sasaki A, Chiba T, Mamiya Y, Otsuki E. Dielectric and piezoelectric properties of  $(\text{Na}_{0.5}\text{Bi}_{0.5})\text{TiO}_3$ – $(\text{K}_{0.5}\text{Bi}_{0.5})\text{TiO}_3$  systems. *Jpn J Appl Phys* 1999;38:5564–7.
- [8] Fu P, Xu ZJ, Chu RQ, Li W, Zang GZ, Hao JG. Piezoelectric, ferroelectric and dielectric properties of  $\text{La}_2\text{O}_3$ -doped  $(\text{Na}_{0.5}\text{Bi}_{0.5})_{0.94}\text{Ba}_{0.06}\text{TiO}_3$  lead-free ceramics. *Mater Des* 2010;31:796–801.
- [9] Zhou XY, Gu HS, Wang Y, Li WY, Zhou TS. Piezoelectric properties of Mn-doped  $(\text{Na}_{0.5}\text{Bi}_{0.5})_{0.92}\text{Ba}_{0.08}\text{TiO}_3$  ceramics. *Mater Lett* 2005;59:1649–52.
- [10] Zuo RZ, Ye C, Fang XS, Li JW. Tantalum doped  $0.94\text{Na}_{0.5}\text{Bi}_{0.5}\text{TiO}_3$ – $0.06\text{BaTiO}_3$  piezoelectric ceramics. *J Eur Ceram Soc* 2008;28:871–7.
- [11] Zuo RZ, Su S, Wu Y, Fu J, Wang M, Li LT. Influence of A-site nonstoichiometry on sintering, microstructure and electrical properties of  $(\text{Bi}_{0.5}\text{Na}_{0.5})\text{TiO}_3$  ceramics. *Mater Chem Phys* 2008;110:311–5.
- [12] Zhao ML, Wang CL, Wang JF, Chen HC, Zhong WL. Enhanced piezoelectric properties of  $(\text{Bi}_{0.5}\text{Na}_{0.5})_{1-x}\text{Ba}_x\text{TiO}_3$  lead free ceramics by sol–gel method. *Acta Physica Sinica* 2004;53:2357–62.
- [13] Pookmanee P, Rujijanagul G, Ananta S, Heimann Robert B, Phanichphant S. Effect of sintering temperature on microstructure of hydrothermally prepared bismuth sodium titanate ceramics. *J Eur Ceram Soc* 2004;24:517–20.
- [14] Jing XZ, Li YL, Yin QR. Hydrothermal synthesis of  $(\text{Na}_{0.5}\text{Bi}_{0.5})\text{TiO}_3$  fine powders. *Mater Sci Eng B* 2003;99:506–10.
- [15] Van-Hal HAM, Groen WA, Maassen S, Keur WC. Mechanochemical synthesis of  $\text{BaTiO}_3$ ,  $(\text{Na}_{0.5}\text{Bi}_{0.5})\text{TiO}_3$  and  $\text{Ba}_2\text{NaNb}_5\text{O}_{15}$  dielectric ceramics. *J Eur Ceram Soc* 2001;21:1689–92.
- [16] Hou JG, Qu YF, Ma WB, Shan D. Synthesis and piezoelectric properties of  $(\text{Na}_{0.5}\text{Bi}_{0.5})_{0.94}\text{Ba}_{0.06}\text{TiO}_3$  ceramics prepared by sol–gel auto-combustion method. *J Mater Sci* 2007;42:6787–91.
- [17] Mercadelli E, Galassi C, Costa AL, Albonetti S, Sanson A. Sol–gel combustion synthesis of BNBT powders. *J Sol–Gel Sci Technol* 2008;46:39–45.
- [18] Xu Q, Chen M, Chen W, Liu HX, Kim BH, Ahn BK. Effect of CoO additive on structure and electrical properties of  $(\text{Na}_{0.5}\text{Bi}_{0.5})_{0.93}\text{Ba}_{0.07}\text{TiO}_3$  ceramics prepared by the citrate method. *Acta Mater* 2008;56:642–50.
- [19] Wang XX, Chan HLW, Choy CL. Piezoelectric and dielectric properties of CeO<sub>2</sub>-added  $(\text{Na}_{0.5}\text{Bi}_{0.5})_{0.94}\text{Ba}_{0.06}\text{TiO}_3$  lead-free ceramics. *Solid State Commun* 2003;125:395–9.